

Electronic Supplementary Information

Wurtzite CZTS nanocrystals and their phase evolution to kesterite thin film for solar energy harvesting

Uma V. Ghorpade^{a,b}, Mahesh P. Suryawanshi^a, Seung Wook Shin^c, Chang woo Hong^a, Inyoung Kim^a, Jong. H. Moon^a, Jae Ho Yun^d, Jin Hyeok Kim^{a*}, Sanjay S. Kolekar^{b*}

^aDepartment of Materials Science and Engineering and Optoelectronics Convergence Research Centre, Chonnam National University, 300, Yongbong-Dong, Buk-Gu, Gwangju 500-757, South Korea

^bAnalytical Chemistry and Material Science Research Laboratory, Department of Chemistry, Shivaji University, Kolhapur 416-004, India

^cCenter for Nanomaterials and chemical Reactions, Institute for Basic Science, Daejeon 305-701, Korea

^dPhotovoltaic Research Group, Korea Institute of Energy Research, 71-2 Jang-Dong, Yuseong-Gu, Daejeon 305-343, South Korea

1 Experimental Section

Chemicals

Copper chloride (CuCl_2 , 99.99%), zinc chloride (ZnCl_2 , 99.99%), tin chloride (SnCl_2 , 99.99%), thiourea ($\text{CH}_4\text{N}_2\text{S}$, 99.99%), ethylene glycol (EG) ($\text{C}_2\text{H}_6\text{O}_2$, 99.99%), Zn acetate, CdSO_4 , Ammonia and ethanol ($\text{C}_2\text{H}_5\text{OH}$, 99.99%) of analytical grade were purchased and used as received from Sigma Aldrich.

Synthesis of CZTS nanocrystals

In a typical experimental synthesis, 1.5 mmol CuCl_2 , 0.75 mmol ZnCl_2 and 0.75 mmol SnCl_2 were dissolved in EG solution into three - naked flask with a constant stirring. The solution was allowed to evacuate under inert atmosphere for 10 min. The precursor solution was heated at 130 °C. The color of the solution changes from cream white to faint green that may indicates the formation of metal-glycol complex. The sulfur source was used by dissolving 3 mmol of thiourea separately into the 50 ml EG. This solution was then hot injected into the metal precursor solution at 130 °C and temperature further allowed to rise at 190 °C. After every 1h, aliquots were taken out from the reaction solution and then cooled at room temperature. A volume of 10 ml ethanol was added into the aliquots and NCs were collected by centrifugation at 3000 rpm for 10 min. After washing by another two volumes of 10 ml ethanol and centrifuging, the final NCs were collected. The material was used for further characterization after drying at 60 °C under vacuum. The resulting NCs were further used for thin film formation.

Color evolution

During the typical growth process, the color of solution (Figure S4) gradually changed from initial cream white (after 20 min) to faint green (after 30 min) which ascribe to the formation of metal-glycol complex (metal chelate). Afterwards, this faint green color changes into the brown shade (after 45 min) after the injection of thiourea solution which leads to the formation of binary and ternary sulfides. Eventually, the appearance of black color observed owing to the initiation of CZTS formation from binary and ternary sulfides leads to the nucleation and growth through the Oswald ripening process.

Ink formulation

The behavior of glycol mediated CZTS NCs is optimized for the stable ink formation in ethanol. Numbers of observations were made to check the solubility of CZTS NCs in an appropriate solvent. The CZTS NCs dispersed in toluene, pyridine, and hexanethiol separate out and settle down, whereas the as-synthesized CZTS NCs were easily dispersed into the ethanol as shown in Figure S1. The ethanol dispersion of the NCs has high stability and it even remains unchanged after being stored for a week. In typical ink formulation method, the ink dispersion is made in the proportion of 0.1 mg/ml. This dispersion is then allowed for a magnetic stirring (5 h) followed by the ultra-sonication for 10 min. Following 10 min of sonication to aid mixing, film was spin coated with 2000 rpm for 20 s and used for the further procedure.

2 Device fabrication

The annealed absorber films were processed into photovoltaic devices following standard procedures including chemical bath deposition of CdS (~65 nm), RF sputtering of i-ZnO (~75 nm) and Al-ZnO (AZO) (~500 nm), and DC sputtering of a patterned Al grid as the top electrode. The final devices (2.5 cm x 2.5 cm) were mechanically scribed into cells with an active area of 0.31 cm^2 .

Chemical bath deposition of CdS thin film

Buffer layer of CdS were prepared on CZTS absorber layer by CBD in a hot alkaline medium. The reaction solution was prepared by using CdSO_4 and Thiourea solution and pH was adjusted to 11 by Ammonia solution. The absorber thin film was then immersed in a reaction bath maintained at 80 °C for 13 min. After the deposition, the films were removed from the reaction bath, rinsed with distilled water and dried in air and preserved in an air tight container containing silica gel. The thickness of the deposited buffer layer was ~ 65 nm.

RF magnetron sputtered deposited i-ZnO and AZO

The i-ZnO and 2% Al doped ZnO (AZO) thin films were prepared on SLG/Mo/CZTS/CdS substrate using RF magnetron sputtering system. The ZnO target was made from high purity ZnO powder (99.99%) and the doped AZO target was made from high purity ZnO powder (99.99%) doped with the desired amount of high purity Al_2O_3 powder (99.99%), respectively. The above CdS deposited films were

dried again by blowing with N₂ gas (99.99%) before being introduced into the sputtered chamber. The chamber was evacuated to a base pressure of 4.9×10^{-6} Torr. High purity Ar gas (99.99%) was used as the plasma source and the gas flow rate was controlled at 40 sccm using a mass flow controller. A RF power of 175 W and working pressure of 6 mTorr was used for the deposition. After (i-ZnO/AZO) film deposition, SLG/Mo/CZTS/CdS/(i-ZnO/AZO) substrates will be used for next step.

DC magnetron sputtered deposited Al grid

Prior to the deposition, the chamber was initially evacuated to a base pressure of 5×10^{-5} Torr. High purity Ar gas (99.99%) was used as the plasma source and the gas flow rate was controlled at 50 sccm using a mass flow controller. A DC power of 95 W and working pressure of 5×10^{-5} Torr was used for the deposition. After Al grid deposition, the solar cell structure was finished by mechanical scribing (total cell area without front grid area ~ 0.31 cm²). The photo image of solar cell device fabricated using optimized absorber layer is shown in the Figure S15 (d).

3 Characterization

The structural properties of CZTS NCs and thin film were examined by X-ray powder diffractometer and high-resolution X-ray diffraction (PXRD, PANalytical, X'Pert-PRO, Netherlands and XRD, X'pert PRO, Philips, Eindhoven, Netherlands) operated at 45 kV and 40 mA and 40 kV and 30 mA, respectively and the Raman spectroscopy recorded using Raman microscope (LabRam HR8000 UV, (Horiba Jobin-Yvon, France), KBSI, Gwangju center) with excitation wavelength 514 nm for identification purpose and to assess the phase purity. The surface morphology was observed using Field emission scanning electron microscopy (FE-SEM, Model Hitachi S 4800, Japan). The elemental mapping images and the compositional ratios of the NCs were analyzed by an energy-dispersive X-ray spectra (EDS) attached to the field emission scanning electron microscope (FE-SEM, Model Hitachi S 4800, Japan) measured at Korean Basic Science Institute. To determine the size and morphology of the NCs, the bright-field (BF) transmission electron microscopy (TEM), their corresponding selected area electron diffraction (SAED) patterns, and high-resolution (HR) TEM was carried out using JEOL-3010 at an operating voltage of 300 kV. The chemical binding energy of as synthesized NCs was examined using a high-resolution X-ray photoelectron spectroscopy (HR-XPS, VG Multi lab 2000, Thermo VG Scientific, UK) at room temperature. The binding energies were calibrated using the carbon 1s line at 285.0 eV. The optical properties of the samples were measured by using UV-Visible spectrophotometer (Cary 100, Varian, and Mulgrave, Australia). The photo conversion efficiency and quantum efficiency (QE) for CZTS TFSCs were characterized by a class AAA solar simulator (Sol31, Oriel, USA) and incident photon conversion efficiency measurement unit (PV measurement, Inc., USA) respectively.

Figure S1. Dispersibility of WZ CZTS NCs in various solvents (a) Toluene (b) Pyridine (c) Hexanethiol (d) Ethanol

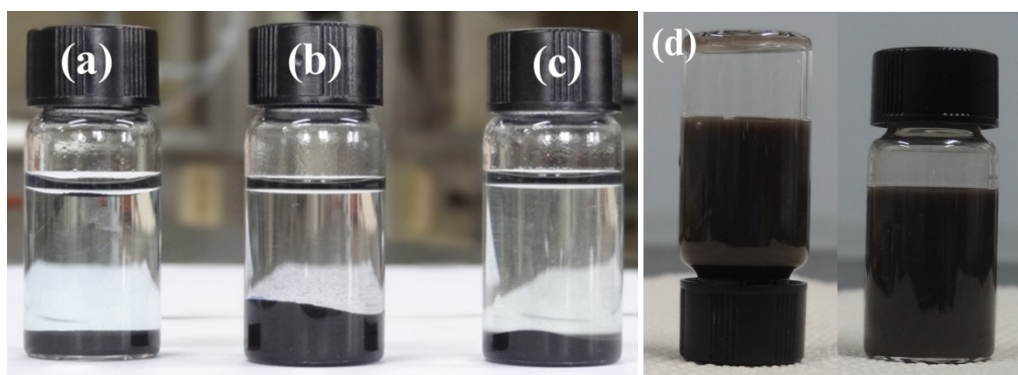


Figure S2. FE-SEM images of WZ CZTS NCs synthesized for 1 h, 2 h, 3 h and 4 h

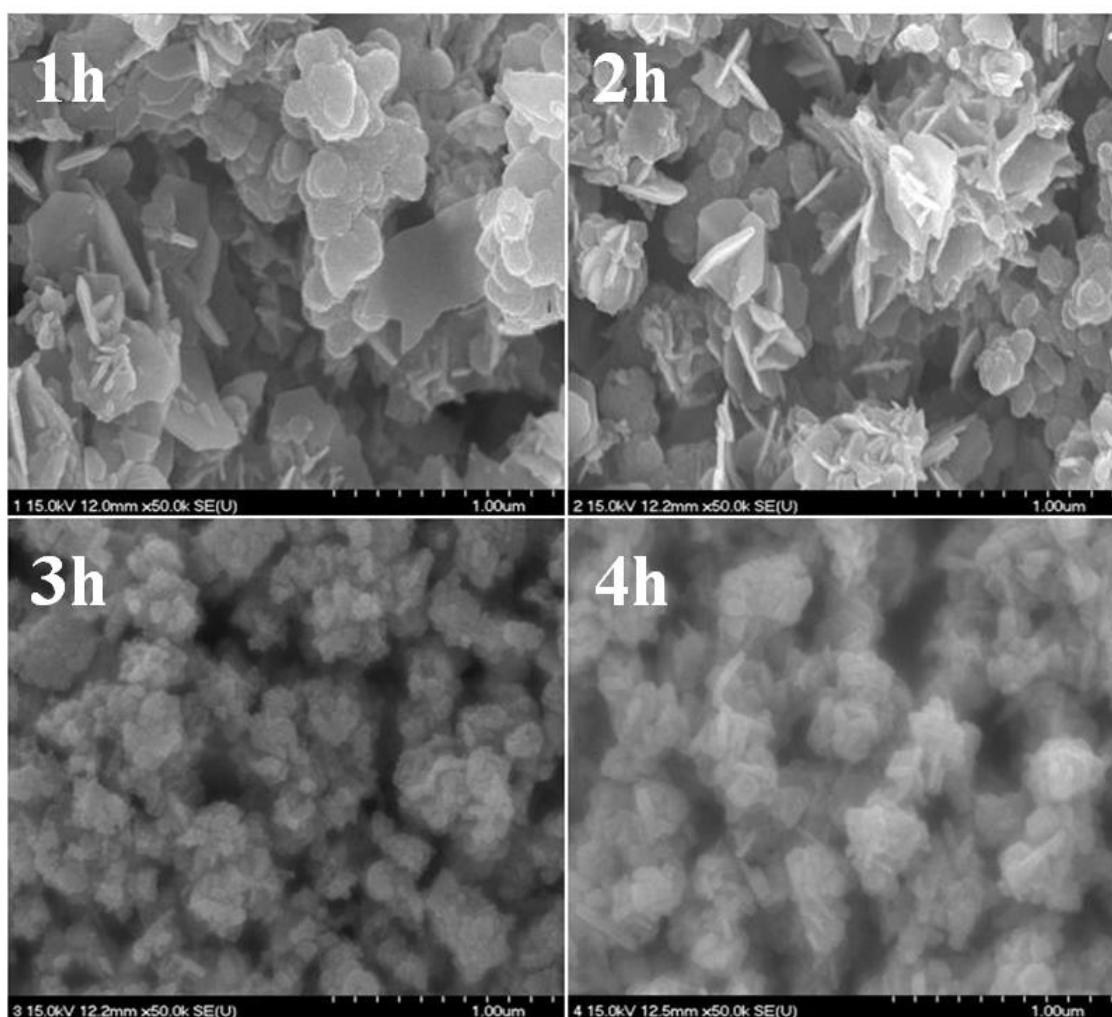


Figure S3. Elemental mapping of WZ CZTS NCs synthesized for 4h

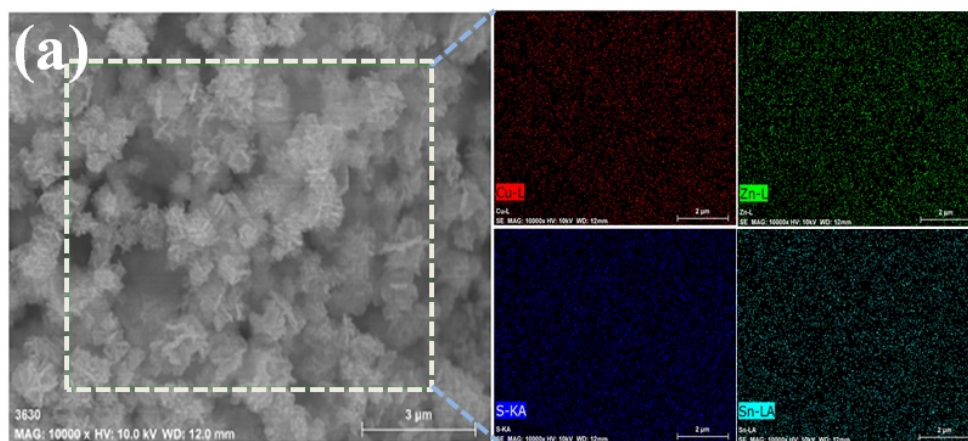


Figure S4. Photographs of reaction solution color evolution during the key intermediates steps of CZTS NCs formation

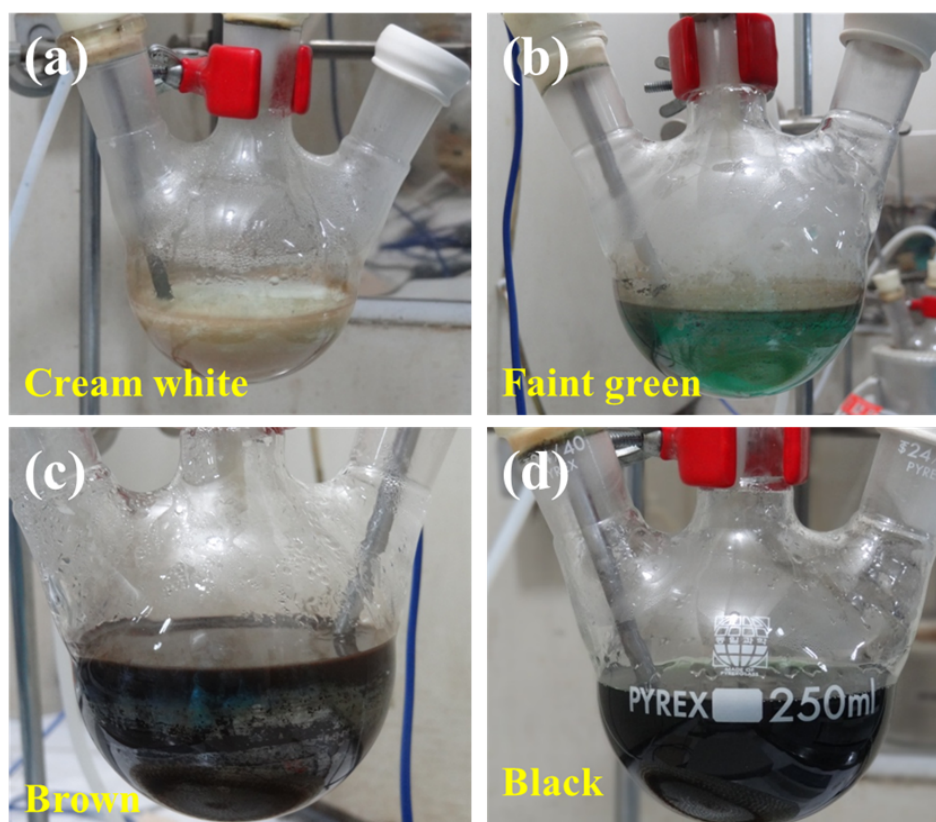


Figure S5. (a) Photograph of an RTA system, (b) Schematic diagram of the sulfurization process in RTA, (c) Photographs of a graphite box used during sulfurization, and (d) Solar cell device of an optimized sample

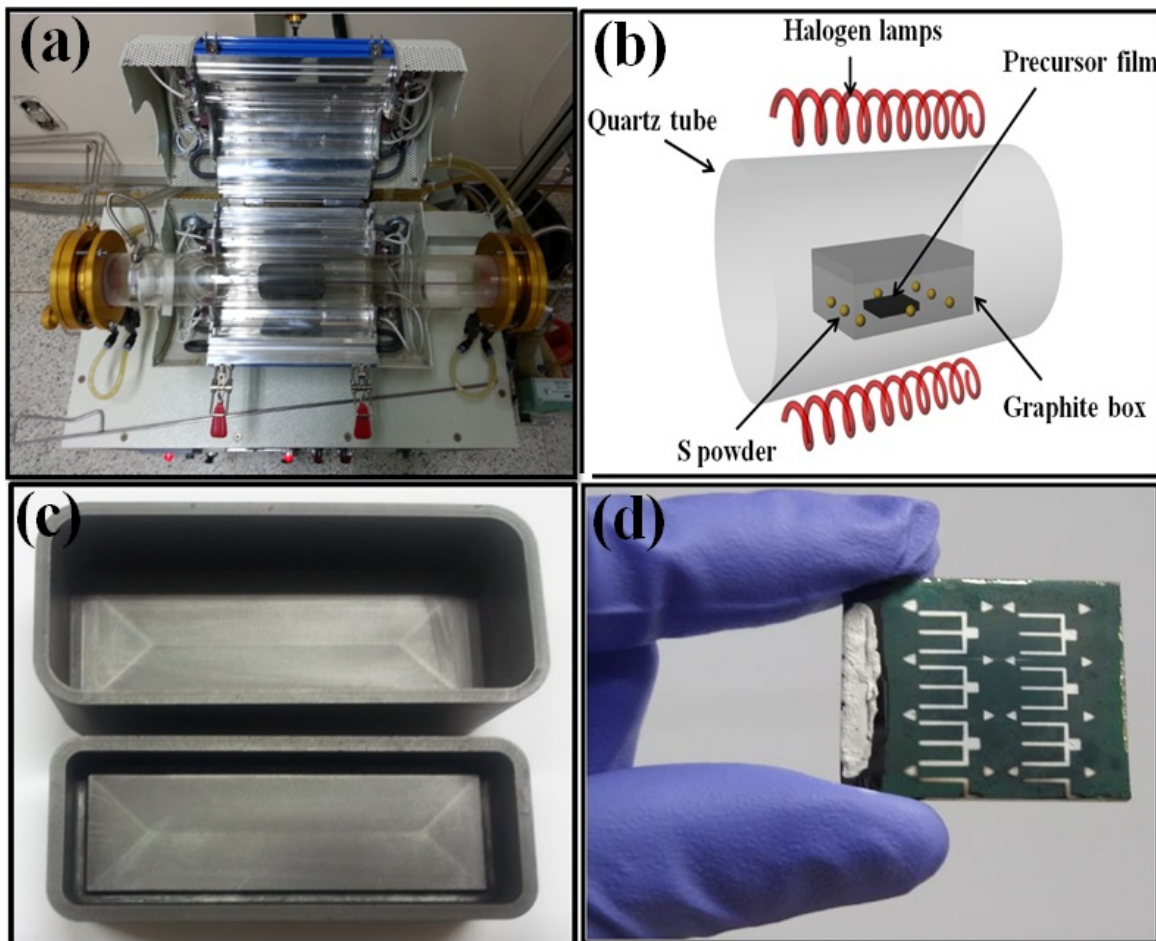


Figure S6. Average photovoltaic performance of six devices from each annealing samples.

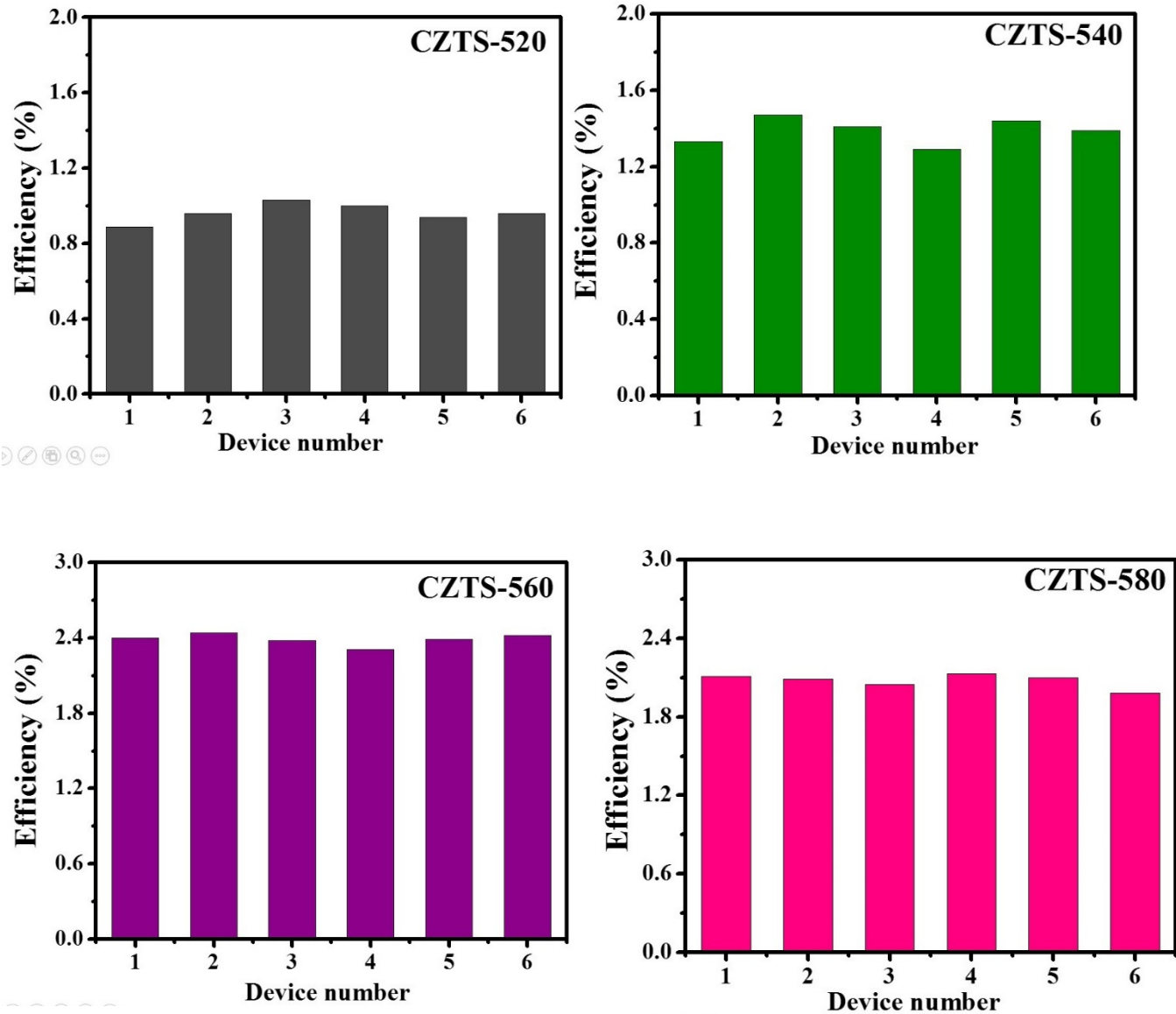


Figure S7 The plots of $[h\nu \ln(1-EQE)]^2$ vs. $(h\nu)$ for CZTS-520, CZTS-540, CZTS-560 and CZTS-580 samples

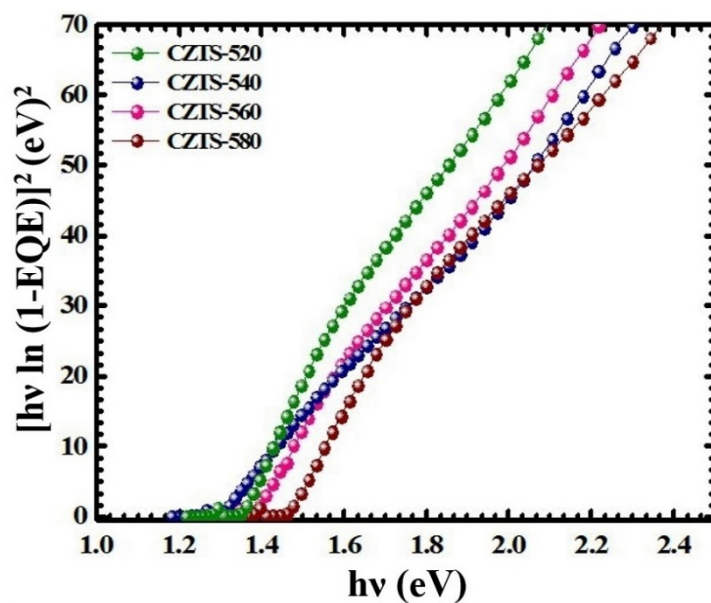


Table S1. Elemental composition of WZ CZTS NCs synthesized for 1h, 2h, 3h and 4h

Samples	Cu	Zn	Sn	S	Cu/(Zn+Sn)	Zn/Sn	S/M
1h	52.89	13.56	6.02	27.66	2.70	2.25	0.38
2h	32.16	13.70	9.91	44.23	1.36	1.38	0.79
3h	26.45	14.81	12.33	46.41	0.97	1.20	0.87
4h	23.97	13.17	12.91	49.95	0.92	1.02	1.00

References

- (1) J. W. Cho, A. Ismail, S. J. Park, W. Kim, S. Yoon and B. K. Min, *ACS Appl. Mater. Interfaces*, 2013, **5**, 4162–4165.
- (2) K. Kim, I. Kim, Y. Oh, D. Lee, K. Woo, S. Jeong and J. Moon, *Green Chem.*, 2014, **16**, 4323-4332.